

Experimental deployment and validation of a distributed SHM system using wireless sensor networks

Nestor E. Castaneda[†] and Shirley Dyke

*Department of Mechanical, Aerospace and Structural Engineering
Washington University in St. Louis, St. Louis, Missouri 63130, USA*

Chenyang Lu, Fei Sun and Greg Hackmann

*Department of Computer Science and Engineering
Washington University in St. Louis, St. Louis, Missouri 63130, USA*

(Received August 28, 2008, Accepted June 29, 2009)

Abstract. Recent interest in the use of wireless sensor networks for structural health monitoring (SHM) is mainly due to their low implementation costs and potential to measure the responses of a structure at unprecedented spatial resolution. Approaches capable of detecting damage using distributed processing must be developed in parallel with this technology to significantly reduce the power consumption and communication bandwidth requirements of the sensor platforms. In this investigation, a damage detection system based on a distributed processing approach is proposed and experimentally validated using a wireless sensor network deployed on two laboratory structures. In this distributed approach, on-board processing capabilities of the wireless sensor are exploited to significantly reduce the communication load and power consumption. The Damage Location Assurance Criterion (DLAC) is used for localizing damage. Processing of the raw data is conducted at the sensor level, and a reduced data set is transmitted to the base station for decision-making. The results indicate that this distributed implementation can be used to successfully detect and localize regions of damage in a structure. To further support the experimental results obtained, the capabilities of the proposed system were tested through a series of numerical simulations with an expanded set of damage scenarios.

Keywords: structural health monitoring; smart sensors; DLAC.

1. Introduction

Emerging interest in the use of wireless sensors for structural health monitoring (SHM) systems is mainly due to the potential of this technology to provide a low cost solution to the damage detection problem through the availability of unprecedented spatial granularity of the response data (Liu and Tomizuka 2003, Spencer 2003, Lynch *et al.* 2002). Most existing SHM techniques require a great deal of high-fidelity response data as well as significant computational power for real-world implementation. Centralized processing of global structural response data has been the norm.

[†] Graduate Research Assistant, Corresponding author, E-mail: necl@cec.wustl.edu

However, a new paradigm is needed to successfully employ wireless sensor networks in this application due to the severe resource and power constraints associated with these networks (Spencer and Nagayama 2006). Properly implemented distributed processing algorithms will significantly reduce the power consumption and bandwidth requirements.

Battery powered smart sensor platforms, based on micro-electro-mechanical systems (MEMS), on-board microprocessors and wireless communication attributes have become a new possibility for developing SHM systems based on distributed processing and wireless sensor networks (WSN). In addition to simply recording response data and transmitting it to a base station, more advanced smart sensors offer powerful on-board processing capabilities that are critical for the distributed computations needed. On-board microprocessors are used to accomplish data aggregation as well as self-operative functions. Wireless communication enables the sensors to then transmit a reduced set of processed information for additional analysis. Lynch provided a comprehensive overview of the last decade of work to develop smart sensor platforms suitable for structural applications (Lynch 2004, Lynch and Loh 2006). Although a number of platforms have been developed in recent years, the Intel iMote2 has emerged as the most appropriate for civil infrastructure monitoring under intensive conditions due to the on-board processing capabilities (Adler *et al.* 2005, Nagayama *et al.* 2006, Nagayama 2007). Additionally, researchers have developed services for this platform that are now publicly available (Rice *et al.* 2008, The Illinois SHM Services Toolkit 2008).

Despite these efforts, practical utilization of smart sensor platforms for SHM in a real-world environment remains a challenge. Power limitations restrict their useful lifetime and performance. Time synchronization is often needed to obtain useful data for SHM applications (Elson *et al.* 2002, Ganeriwal *et al.* 2003, Lynch *et al.* 2005, Maroti *et al.* 2004, Mechitov *et al.* 2004), effective communication protocols are needed for reliable data transmission (Mechitov *et al.* 2004). Thus, middleware services are required to maximize the lifetime of these smart sensors networks and ensure a reliable performance. (Spencer and Nagayama 2006, Nagayama *et al.* 2006, Nagayama 2007) identified a more comprehensive set of research gaps in the development of SHM systems based on smart sensors.

Robust damage detection algorithms, capable of functioning within the confines of a wireless sensor network, continue to pose a significant research problem to the community. Several techniques involving sophisticated and fault tolerant algorithms for damage detection are being studied (Sohn *et al.* 2004, Lynch 2004). For instance, at Clarkson University researchers have implemented a wireless sensor system for modal identification of a full-scale bridge structure in New York (Gangone *et al.* 2007). Battery powered wireless sensor nodes equipped with accelerometers and strain transducers are used having a high wireless data transmission rate. The entire network is polled by a master computer that collects acceleration and strain data. Both modal identification and quantification of static responses is performed using centralized network architecture.

In another real-world wireless sensor application, at the University of California, Berkeley (Kim 2005, Kim 2007, Kim *et al.* 2007, Pakzad *et al.* 2005) researchers have designed and deployed a wireless sensor network on the Golden Gate Bridge. The purpose of this implementation was to validate theoretical models and previous studies of the bridge. The deployment, considered the largest smart sensor network for SHM purposes, involves 64 nodes carefully distributed over the span and the tower measuring ambient vibrations synchronously at 1kHz in two directions. The data, reliably transmitted by using a 46 hop network with a bandwidth of 441B/s at the 46th hop, is collected using a base station (i.e., centralized network architecture) where frequency domain

analysis is used to extract modal parameters. The total time required to transmit response data from all nodes to the base station is 9 hours, resulting in a system lifetime of 10 weeks when four 6V batteries are used as a power source.

Other smart sensor applications in infrastructure systems have been reported. At the University of Oklahoma researchers have conducted and presented preliminary results for an experimental investigation to detect road weather conditions using a smart sensor network (Pei *et al.* 2006, Ferzli *et al.* 2006). In the implementation, a network of Mica2 motes, interfacing with three environmental sensors, are deployed to monitor pavement temperature and moisture to detect icy road condition. Sensed data, transmitted across the network and collected at a base station, is subsequently processed to categorize pavement surface conditions. In the study, several experiments were also performed to test communication interference due to traffic using a small-scale sensor network in a pseudo-field environment.

Clearly, with potentially hundreds of nodes sensing and streaming data at high sampling rates, the energy consumption and power requirements of these centralized approaches do not match the capabilities offered by wireless sensors, and therefore are not scalable for realistic SHM applications. The development of distributed approaches that minimize data transmission, and thus power consumption, is necessary. On-board processing capabilities using wireless sensors are successfully being exploited to perform data aggregation, thus reducing the wireless communication load (Lynch *et al.* 2004, Chintalapudi *et al.* 2006, Nagayama 2007, Hackmann *et al.* 2008, Zimmerman *et al.* 2008).

A distributed approach, amenable for local processing in the motes, has been proposed by Chintalapudi *et al.* (2006). In this study, two qualitatively different SHM applications for damage detection and localization are tested using a small and medium-scale structures and NetSHM prototype. The damage detection was accomplished by analyzing shifts in modal frequencies, while damage localization based on mode shape changes. However, due to memory and processing capacity constraints in the platform (MicaZ), the technique evaluation was performed without involving any local processing on the smart sensors.

At the University of Michigan, Lynch *et al.* have developed a state-of-the-art wireless sensing unit configured with an autonomous execution of an embedded damage detection algorithm based on statistical pattern recognition using AR and ARX time-series models (2004). The algorithm performance is evaluated using wireless sensor units and experimental data previously acquired with an accelerometer network deployed on a simple lumped-mass laboratory test structure. Final results demonstrated that a fifty percent reduction in energy was reported by running the damage detection scheme at the sensor nodes as compared to using a centralized approach.

Zimmerman *et al.* have also implemented a distributed WSN for modal identification by appropriate implementation of select output-only methods (peak-picking, frequency domain decomposition, random decrement) (2008). Their implementation, tested on a theater balcony, uses a parallel data processing and reduced communication scheme to ensure scalability and power efficiency in the network. Three network topologies are proposed to yield a two-node data sharing chain for global mode shape identification by combining partial identified mode shapes. However, there is a potential for significant accumulation of errors with this strategy, if any of the sensor nodes acquires unreliable data.

Additionally, researchers at the University of Illinois at Urbana-Champaign have experimentally validated a distributed SHM system employing a smart sensor network deployed on a scale three-dimensional truss model (Spencer and Nagayama 2006, Nagayama 2007). Their approach includes

implementation of the Distributed Computing Strategy (Gao 2005) in which data is processed on iMote2 smart sensor communities under a hierarchical architecture. The algorithm includes the use of the eigensystem realization algorithm (Juang and Pappa 1985) and the damage locating vector method (Bernal 2002) to exploit the on-board processing capacity of the iMote2. Results demonstrated that the adopted SHM system is effective for damage detection and localization, and is scalable to a large number of smart sensors. However, significant communication is needed when cross-correlation tasks are performed, resulting in considerable energy consumption in the network.

The focus of this work is the development and experimental validation of a completely distributed damage detection system that has minimal power requirements and will be effective for identification of damage zones in a structure. The communication load and power requirements are considerably reduced by exploiting the local processing capabilities offered by the wireless sensors. Nearly all computation is performed on-board the sensor platforms, and a minimal amount of data must be transmitted to a base station for decision-making. The system is based on the use of the DLAC method, developed by Messina *et al.* (1996) and first proposed for wireless sensor networks by Clayton *et al.* (2005). The implementation of this distributed processing algorithm on the smart sensors is discussed. One additional advantage of this approach is that synchronized sensing is not needed. The system is deployed and validated on two experimental structures of increasing complexity using a WSN based on iMote2 platforms. With very little energy usage the system is experimentally demonstrated to be capable of detecting the damage zone.

2. Description of the distributed processing implementation

The proposed damage detection system is implemented using a WSN. A two-level approach is used where level one involves data aggregation performed on the sensors, and level two yields damage localization results at the base station. The system is completely distributed (all sensors operate independently of each other) and is based on correlation of the changes in the natural frequencies of the experimental structure and an analytical model. In this approach minimal power is expended at the sensor level because the information transmitted is reduced by several orders of magnitude.

A general flow chart of the entire implementation is provided in Fig. 1. The level one analysis identifies the natural frequencies of the structure using the onboard processing abilities of the smart sensor platform. A reduced set of parameters are then transmitted to the base station. At the base station, the second level analysis is then performed to determine the correlations and localize damage. A Java program has been developed as an interface to set experimental parameters and govern which tasks are to be conducted within the experiment.

The steps performed in the damage detection system include: i) data acquisition, ii) on-board data processing, iii) data transmission and damage localization at the base station. These will be described in the following sections. The user interface for controlling the experiment is also described herein.

2.1 Data acquisition

Acceleration data acquisition is performed as a first step through the proposed damage detection

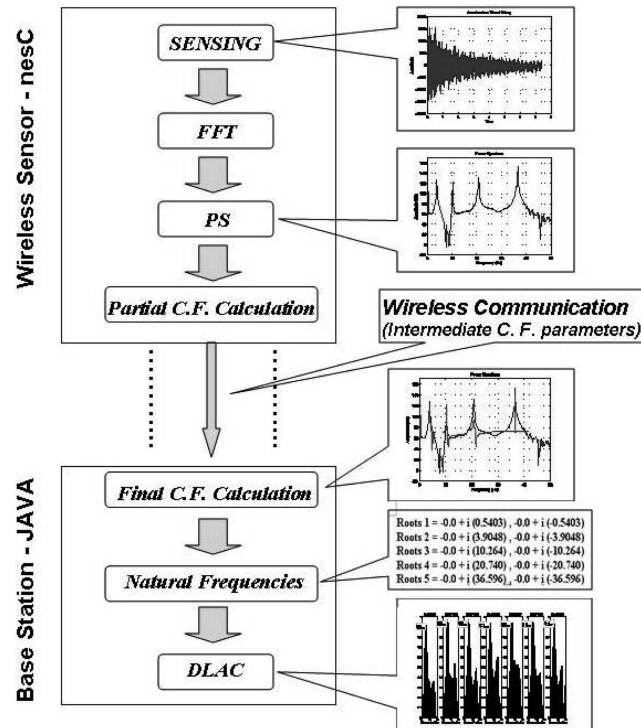


Fig. 1 Flow chart of implementation

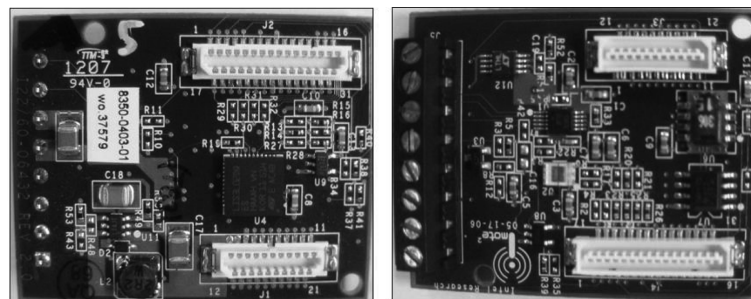


Fig. 2 Top and bottom view of basic sensor board

system to be used to identify the natural frequencies of the structure. A basic sensor board (ITS400) developed by Intel Research Lab and designed to interact with the *iMote2* platform is used to accomplish the acceleration measurement.

The basic sensor board has a digital accelerometer with additional temperature, humidity and light sensors. Four A/D converters are available for the sensors. The digital accelerometer (ST Micro LISL02DQ) with 3-axes of measurement has a resolution of 12-bits, or equivalently 0.97 mg of resolution based on the ± 2 g range. A limit of 3000 data points may be obtained on each axis. A photo of the basic sensor board is shown in Fig. 2.

Acceleration data is collected at a specific sampling frequency within frames each containing 2048 points. The raw data are then stored in the local memory of the *iMote2*. The program running

Table 1 Accelerometer user specified sampling rates and cutoff frequencies

Decimation factor	Cutoff frequency (Hz)	Sampling rate (Hz)
128	70	280
64	140	560
32	280	1120
8	1120	4480

on each of the motes (implemented in the *nesC* programming language) is designed to process the acceleration data to perform modal identification. Sampling frequencies and corresponding cut-off frequencies are adjustable and are set using the digital filters and user-defined decimation factors with values given in Table 1. Specifications available for the accelerometer explain that once the decimation factor is defined, the sampling frequency and resultant cut-off frequency will have a value within $\pm 10\%$ of the value set by the user.

For instance, if a decimation factor were defined as 64, the sensor would operate with an actual sampling frequency between 504-616 Hz (i.e., not precisely at 560 Hz). Consequently, sampling frequency values will vary from sensor to sensor. The actual values could be determined using an oscilloscope prior to experimentation or by a self-calibration routine embedded in the smart sensors. However, on a given sensor a consistent sensing frequency was observed (i.e., there was no variation in the sampling frequency value with time).

2.2 Data processing

Modal identification is performed on each smart sensor. A Fast Fourier Transform (FFT) is first applied to the acceleration time histories on the sensor platforms. Power spectral density (PSD) functions are then calculated as the squared magnitude of the complex FFT values. Assuming that the unmeasured disturbances to the structural system are white noises and have flat PSDs, the PSD of the response can be viewed as a transfer function. Even in the case when the input is not white, this approximation has been found to be appropriate for determination of the frequencies of the system using the method discussed subsequently. Data obtained with each sensor is processed entirely at that particular sensor node and no transmission of the raw data is needed to implement the algorithm.

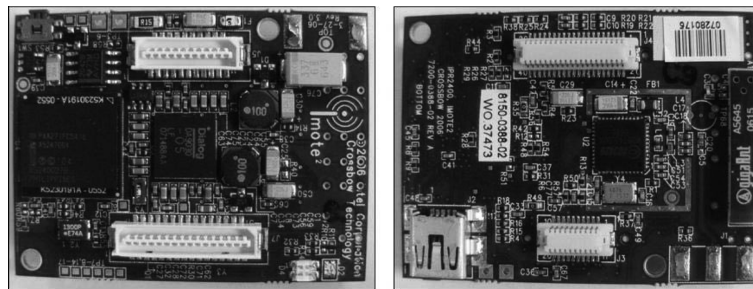
A curve fitting technique is applied to the PSD function to determine the values of the frequencies. A fit of the PSD data immediately surrounding each of the modes is performed to identify each frequency. Levi's approach is used to accomplish the curve fitting (Levy 1959). This approach was proposed in prior related studies (Clayton *et al.* 2005, Clayton *et al.* 2006, Clayton, 2006). The approach identifies the natural frequencies by determining the parameters that result in a least-squares fit of a fractional polynomial expression to the frequency domain data. The fractional polynomial is defined as the ratio of two complex polynomials in terms of unknown coefficients a_i , b_i , as in Eq. (1)

$$G(i\omega) = \frac{a_0 + a_1(i\omega) + a_2(i\omega)^2}{b_0 + b_1(i\omega) + b_2(i\omega)^2} \quad (1)$$

Because we are fitting the data in the region surrounding each peak, the denominator has a polynomial order of two, i.e., equal to two times the number of frequencies to be captured. The

Table 2 *iMote2* main board properties

Microprocessor	XscalePXA271
Active power (mW)	44 @ 13 MHz, 570 @ 416 MHz
Clock speed (MHz)	13 - 416
RAM (bytes)	256 K + 32 M external
Program flash (bytes)	32 M
802.15.4 radio (Chipcon 2420)	

Fig. 3 Top and bottom view of *iMote2* main board

curve fit procedure is repeated for each of the modes to be identified. The set of coefficients defining the results of the curve fit are then transmitted wirelessly to the base station where natural frequencies are calculated from the imaginary component of the roots of each denominator polynomial, i.e., the poles of the system.

The *iMote2* (IPR2400), an advanced wireless sensor platform which offers adequate processing power to accomplish the FFT, PSD and curve fitting tasks, is selected for this study. Its main board has a low power 416MHz PXA271 XScale processor with 256 KB of integrated SRAM and 32 MB of external SDRAM, embedded in a modular compact size of $48 \times 36 \times 7$ mm. Power can be provided by a battery board or via the integrated USB interface. Other important *iMote2* main board features can be observed in Table 2. This choice of smart sensor platform made it possible to implement this completely distributed approach for structural damage detection. A photo of the unit is shown in Fig. 3.

2.3 Data transmission

The set of parameters associated with the model fitted to the PSD and calculated on the sensor platforms and then transmitted back to the base station. These values are transmitted from the *iMote2* to a PC base station wirelessly through a gateway mote.

A gateway mote, receives the data packets from the sensors using an 802.15.4-compliant 2.4 GHz radio (Chipcon CC2420) integrated with a built-in antenna, and relays the data to the PC over a USB cable. The PC base station completes the DLAC computations and provides the results to the user with a Java application.

At this point the communication, latency, and energy consumption advantages presented by the distributed damage detection strategy, implemented in this study, should be highlighted. The evaluation is performed by analyzing the execution time for the computational tasks performed on-

board and the wireless transmission from the sensor to the base station. The corresponding times are measured using the *iMote2* onboard microsecond timer. Additionally, the time incurred to transmit the data from the sensor to a base station under a centralized approach is also measured for comparison purposes. Under a common centralized approach without exploiting the on-board processing capacity offered by the smart sensors, 2048 integer sensor readings would have to be transmitted back to the base station. However, under the proposed distributed approach only partial results consisting of $5n$ floating-point curve fitting parameters (where n is the number of modes to be captured) are transmitted back to the base station for final natural frequencies calculation. For instance, if $n = 5$ then a 98.8% of data reduction is accomplished because only 25 floating-point parameters are transmitted to the base station against the 2048 integer sensor readings. Furthermore, latency analysis demonstrated that the distributed approach only takes 4723 ms among acceleration data collection, processing and aggregation data at sensor level and final wireless transmission tasks. The centralized procedure requires 13410 ms to collect all the raw data and transmit the entire set to the base station. Consequently, the proposed distributed approach is able to achieve latencies 64.8% lower than those of a centralized approach.

Additionally, energy consumption is analyzed using the previous latency analysis results in conjunction with the current consumption data for radio, sensor and CPU provided by the manufacturers (STMicroelectronics 2005, Crossbow Technologies 2007). The results indicate that the presented distributed processing approach reduced the energy usage to 0.067 mAh in contrast to the 0.222 mAh that a centralized approach would require. Therefore, the proposed distributed approach yields an energy reduction of almost 70% of that of the centralized approach. This reduction is mostly attributed to the fact that no raw data is sent to the base station. The distributed approach only requires 0.006 mAh for the on-board computation instead of the 0.160 mAh that it would be needed to transmit the entire raw dataset to the base station under a centralized approach. Therefore, low latency and minimal energy use are demonstrated based on the proposed distributed approach.

Although the purpose of this study is to validate a distributed implementation, raw data is also available to be transmitted to the base station for debugging and comparison analysis. Therefore, a reliable transport layer is implemented to achieve accurate data transmission from wireless sensors to the base station. This reliable transport layer is tailored for the specific features of the *TinyOS 1.1.15* operating system. The transport layer divides sensor data into packets small enough for the radio protocol stack to handle, transmits all the data packets to the base station, and reassembles them upon arrival. Additionally, an Automatic Repeat Request procedure (ARQ) is implemented to detect and retransmit lost packets during communication. After a sender sends a data packet to the base station, it waits for an acknowledgment from the receiver. If an acknowledgment is not received within 0.5 sec it will retransmit the data packet. This process is repeated until an acknowledgment is received, at which time the sender mote proceeds to the next data packet. To detect duplicate data packets, each data packet has a sequence number differentiating it from the other packets. Therefore, the base station accurately reassembles the original block of data after all of the packets are received. The communication protocol was verified experimentally using seven wireless sensors, located 16 feet from the base station. Obstacles such as metal bookcases were placed between the base station and the wireless sensor deployment to observe performance. To detect communication failures, a pattern of bytes was written into the block data before sending it to the base station which is configured to verify if the pattern of bytes still exists after transmission is concluded. The pattern of bytes used was a counter that repeatedly goes from 0x00 to 0xFF.

Through the test, each of the seven *iMote2* wireless sensor sent their block data to the base station sequentially. All of the data from the network arrived successfully, which confirmed the communication protocol is reliable.

2.4 Damage localization

Once the parameters from the curve fit arrive to the base station, the java code at the base station is used to compute the frequencies and calculate correlations to provide to the user. Messina proposed the Damage Location Assurance Criterion (DLAC) (Messina *et al.* 1996, Messina *et al.* 1998) as an adaptation of the Modal Assurance Criterion (MAC) (Contursi *et al.* 1998) technique for damage detection. The DLAC approach can identify damage by evaluating the linear correlation between the frequency change vectors obtained by experimental measurements and an analytical model. Consequently, DLAC requires the selection of an assumed damage detection pattern to produce frequency change vectors for the numerical model. Therefore, the *j*th DLAC coefficient represents the correlation of the frequency change vectors between the experimental natural frequencies and numerical natural frequencies which are produced when the damage detection pattern is imposed on the *j*th element of the numerical model. Damage is inherently nonlinear, but because the structure experiences ambient vibration before and after the damage, linear models are used to represent the structural behavior before and after damage. The experimental natural frequencies are calculated as the imaginary component of the poles of each fractional polynomial as explained in the data processing section. The linear correlation between frequency change vectors is computed using the DLAC equation given by Eq. (2).

$$DLAC_j = \frac{|\{\Delta\omega\}^T \{\delta\omega_j\}|^2}{(\{\Delta\omega\}^T \{\Delta\omega\})(\{\delta\omega_j\}^T \{\delta\omega_j\})} \tag{2}$$

where

$$\Delta\omega = (\omega_{healthy} - \omega_{damage}) / \omega_{healthy} \tag{3}$$

$$\delta\omega_j = (\omega_{healthy}^a - \omega_j^a) / \omega_{healthy}^a \tag{4}$$

ω : Vector of natural frequencies obtained with experimental measurements

ω^a : Vector of natural frequencies obtained with the analytical model

j : DLAC index associated to the *j*th element location in the analytical model

Frequency change vectors for experimental and numerical models are denoted by $\Delta\omega$ and $\delta\omega_j$, respectively. These vectors are normalized with respect to the healthy natural frequencies using Eqs. (3) and (4) to equally weight all vectors and reduce any bias induced by higher modes. Note that the result of this is restricted to positive values between 0 and 1. A concentration of relatively high DLAC values indicates strong correlation and therefore a potential damage location.

Although the DLAC values are dependent on both the level and location of the assumed damage, the DLAC's ability to detect damage is robust, because frequency change vectors are normalized and their magnitude is unnecessary for the calculation. However, some uncertainties present during an actual implementation of the DLAC have been found to affect its reliability (Clayton 2006). Clayton performed an assessment of the DLAC accuracy in previous numerical studies using a



Fig. 4 User-interface

cantilever beam model. In his study it was concluded that the reliability of the DLAC to detect damage is dependent on having a sufficiently refined analytical model. The success of the method is also dependent on the noise distribution present in the output signals. These effects are later considered in a numerical simulation using an analytical model of a truss.

Because the DLAC approach is only used to detect individual damage events, extensions of this technique could be implemented to detect multiple damage locations (Koh and Dyke 2007) or to detect damage in perfectly symmetric structures. Also, a sufficient number of modes must be employed. If the number of modes is not sufficient, the frequency change vector can result in strong correlation with more than one damage pattern, limiting the usefulness of this approach for real structural damage localization.

2.5 Description of user interface

A Java application was also developed as a user-interface to monitor and control the entire network and define the sensing parameters. Fig. 4 shows the user-interface developed for this implementation. The proposed interface enable users to set sampling frequencies for sensor boards, select curve fitting intervals in the frequency domain, initialize the application and save results for post-processing. Additionally, raw and corresponding power spectrum data may be requested and recorded for debugging purposes.

3. Experimental deployment and validation

Experimental deployment and validation of this SHM system is conducted using two experimental structures of increasing complexity. The first structure considered is a simple cantilevered beam. The second deployment focuses on a more complex truss structure. Details on the deployment and experimental validation on these test structures are discussed in this section.

3.1 Cantilivered beam experiment

A steel cantilever beam, located at the Structural Control and Earthquake Engineering Lab at Washington University in St. Louis, is first considered (Clayton *et al.* 2005, Clayton 2006). The beam is 274.3 cm long, 7.6 cm wide and 0.6 cm thick. Seven *iMote2s* platforms are attached to the beam to measure acceleration responses in a direction parallel to the weak axis, placed at constant

intervals of 38.1 cm measured from the base. Sensors are configured to have a sampling frequency of 280 Hz, corresponding to a cutoff frequency of 70 Hz.

A numerical model is developed to yield healthy and damaged analytical natural frequencies for later correlation calculations needed for the DLAC technique.

The model employs 2D Bernoulli beam elements with transverse and rotational degrees of freedom (DOF), producing a consistent mass matrix finite element model with 20 elements and 42 global degrees of freedom (see Fig. 5).

Boundary conditions assume a perfect cantilever support. Using the numerical model, 20 analytical damage scenarios are generated. Analytical damage is produced in the model by increasing the density in the damaged element to represent a mass increase. The amount of mass added at each element is only 67% (1.00 kg) of the true experimental value of the added mass (1.50 kg). The eigen-problem is solved to obtain the healthy natural frequencies and a sensitivity matrix containing information about the first five bending natural frequencies for each of the 20 damage locations on the beam model. Analytical natural frequency results (in Hz) for healthy and damaged natural frequencies are given in Table 3. Three damage scenarios are independently examined using impact testing. Rather than damaging the structure, mass is added in specified locations to change the dynamics of the structure. Thus, each damage scenario is simulated by attaching a steel bar with an equivalent weight of 1.50 kg placed at distances from the base of: 66.0 cm (D1), 134.6 cm (D2), and 189.5 cm (D3), respectively. See Fig. 6 for a diagram of the

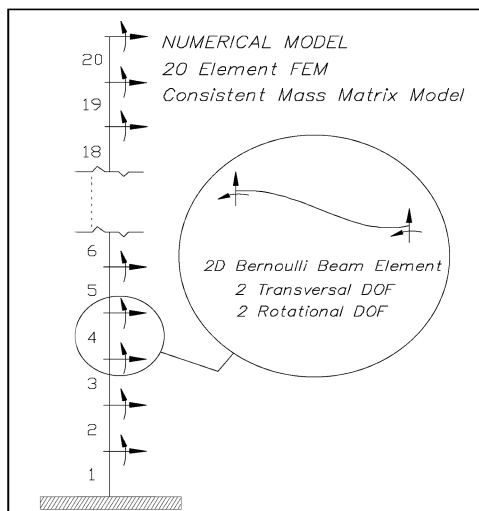


Fig. 5 Cantilever beam finite element model

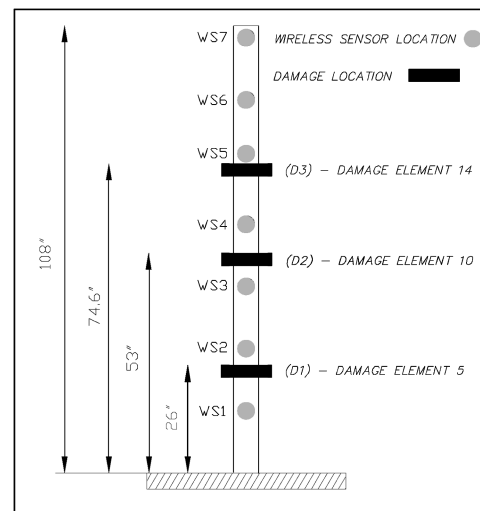


Fig. 6 Diagram of cantilever beam test structure

Table 3 Analytical natural frequencies

Mode	Healthy	D1	D2	D3
1	0.6564	0.6555	0.6443	0.6200
2	4.1133	4.0105	3.7649	4.0026
3	11.5180	10.6192	11.4581	10.7937
4	22.5710	20.8768	21.0991	22.3574
5	37.3160	36.1469	36.8913	36.1677

Table 4 Experimental healthy natural frequencies

Mode	1	2	3	4	5
W_n	0.5381	4.0240	11.4705	22.5506	37.4316

experimental setup. In the experiments the mass is associated with elements 5 (case D1), 10 (case D2) and 14 (case D3) in the model. Therefore, the highest DLAC values are expected to be concentrated around these positions.

The first experimental test is performed to identify the healthy natural frequencies of the beam. A hammer strike is applied along the weaker bending axis of the beam to approximate an impulse response and to ensure a sufficiently broadband excitation. The first five healthy natural frequencies (in Hz), shown in Table 4, were determined by averaging the results obtained from each of the smart sensors. These values are incorporated into the java tools that perform the DLAC computations.

The damage scenario experiments are then performed to test the distributed SHM system. Mass is attached to the beam and impact testing is used to excite the structure for each of the damage scenarios. The results reported by the smart sensor network are provided in Figs. 7, 8 and 9 and the corresponding identified natural frequencies (in Hz) and DLAC measurements are presented for each damage scenario. Recall that the experimental damage cases D1, D2 and D3 are associated with elements 5, 10 and 14, respectively. From these results it is clear that the highest DLAC values correspond directly to the damage location for this simple beam structure.

Mode	WS1	WS2	WS3	WS4	WS5	WS6	WS7
1	0.5506	0.5374	0.5402	0.5316	0.5371	0.5427	0.5392
2	3.9043	3.8902	3.8977	3.8564	3.7678	3.8488	3.9012
3	10.2473	10.2779	10.2714	10.2744	10.0707	10.3217	10.2533
4	20.7641	20.8096	20.7964	20.8470	20.4038	20.7546	20.7751
5	36.6415	36.6396	36.6048	36.6785	35.9797	36.5919	36.6570

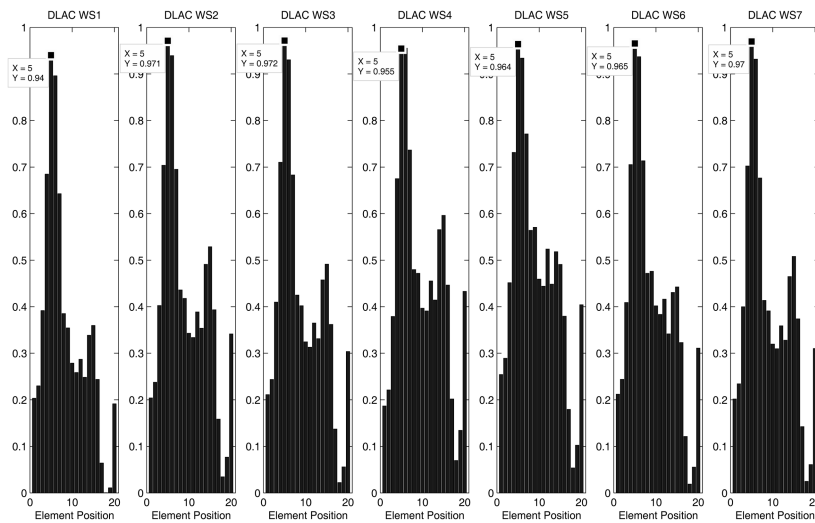


Fig. 7 DLAC results for element position # 5

Mode	WS1	WS2	WS3	WS4	WS5	WS6	WS7
1	0.5498	0.5393	0.5386	0.5318	0.5353	0.5420	0.5379
2	3.6042	3.6241	3.6343	3.5979	3.7358	3.5478	3.6284
3	11.4766	11.4127	11.4758	11.4310	11.2721	11.3961	11.4565
4	20.7626	20.7606	20.7952	20.7798	20.4008	20.7528	20.7586
5	37.2342	37.2030	37.2573	37.2568	36.6449	37.1650	37.2391

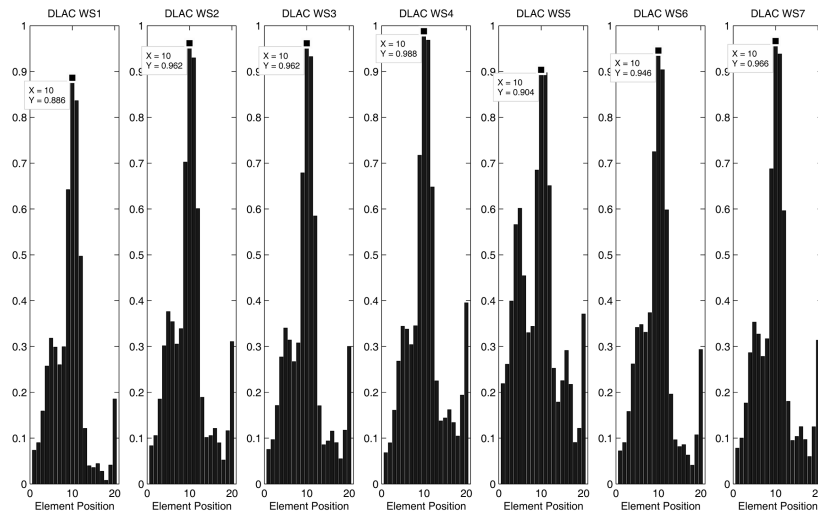


Fig. 8 DLAC results for element position # 10

Mode	WS1	WS2	WS3	WS4	WS5	WS6	WS7
1	0.4767	0.4998	0.5030	0.5167	0.4806	0.4925	0.5101
2	3.8829	3.8889	3.9201	3.8785	3.8450	3.9297	3.9071
3	10.6125	10.6045	10.5549	10.6421	10.4151	10.5883	10.6263
4	22.2777	22.2284	22.2484	22.2936	21.8712	22.2304	22.2407
5	36.4255	36.3849	36.4066	36.4745	35.8035	36.3518	36.4494

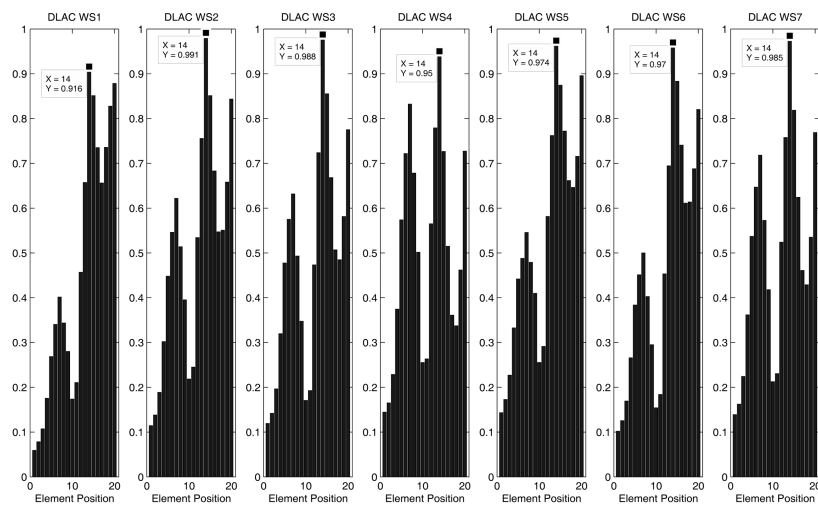


Fig. 9 DLAC results for element position # 14

Despite the accuracy of this approach in localizing damage here, some of the sensors do report similar DLAC values in the final damage scenario (D3). This outcome is a possibility in this approach due to the fact that pattern in the frequency change may be similar for two damage scenarios. Using more frequencies in the DLAC method would likely correct this error, but at this time are outside of the bandwidth of the sensors. However, this method is found to be robust to the level of damage assumed for DLAC determination, requires only a few modes for implementation, and has not been found to result in false negatives; locations indicating high levels of correlation do include the damage location.

3.2 Truss experiment

A steel truss structure is selected as a second, more complex experimental model for validation of the proposed SHM system (Clayton 2002, Gao 2005, Nagayama 2007). This model is housed in the Smart Structure Technology Laboratory (SSTL) at the University of Illinois at Urbana-Champaign (see Fig. 10) and has been the subject of several SHM studies in the past. The specimen, with 5.6 m long, has 14 bays each 0.4 m in length and depth, and rests on four rigid supports. Two of these supports, located at one end of the truss, are pinned and are able to rotate freely with all three translations constrained. The other two supports, located at the other end of the truss, have rollers and are able to translate only in the longitudinal direction of the truss. Each of the truss members has a tubular cross section with an inner diameter of 1.09 cm and outer diameter of 1.71 cm and

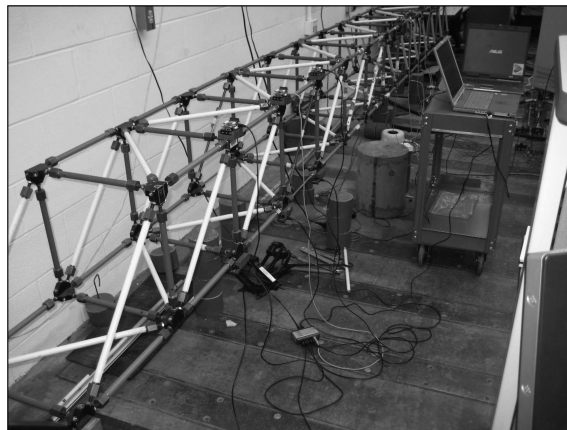


Fig. 10 3D truss test structure

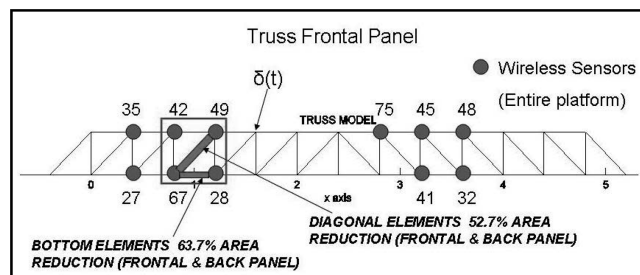


Fig. 11 Truss experiment set up

can be removed or replaced for simulating damage without disassembling the entire structure.

In our implementation a network of eleven *iMote2* wireless sensor platforms is deployed on the front panel of the truss as indicated in Fig. 11. Sensor boards are configured to measure vertical acceleration data with a sampling frequency of 560 Hz which corresponds to a cutoff frequency of 140 Hz. Sensors are oriented in the vertical direction to focus on measuring bending modes of the structure.

A numerical model is developed to produce the necessary frequency change vectors for the DLAC computations. 3D Bernoulli beam elements are used with transverse, rotational, torsion and axial degrees of freedom to produce a consistent mass matrix finite element model with 160 elements and 336 global degrees of freedom (see Fig. 12). Boundary conditions are modeled in agreement with the actual boundary conditions of the truss. Three translational and three rotational degrees of freedom are defined for each structural node and an additional mass of 1 kg is lumped at every translational DOF to account for inertial effects introduced by the steel joints. An effective experimental damage scenario is performed by replacing four members of the third central bay on both the front and rear truss panels as shown in Figs. 11 and 12. Diagonal members are replaced with members having a reduced area of 52.7% or the original and bottom chord elements are replaced with members having a reduced area of 63.7 % of the original.

Damage patterns corresponding to a reduction in the area of the diagonal and bottom elements in each of the 12 central bays are then reproduced in the analytical model. Here the actual experimental damage is applied by modeling the same section reduction. Therefore, for the experiments a damage hypothesis identical to the actual damage is used to produce a damage detection pattern for correlation comparisons. However, modeling errors are included in the analysis as the analytical model of the truss has not been updated to reflect the healthy condition of the structure. Analytical natural frequency results (in Hz) for healthy and damage cases are depicted in Table 5. A frequency change vector that includes the first five bending natural frequencies over each of the 12 damage scenarios is calculated. Note that according to the true damage patterns, the highest DLAC values are expected to be concentrated around to the third bay due to the presence of damage.

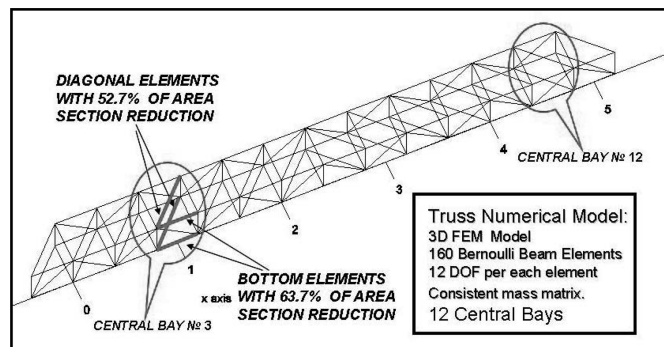


Fig. 12 Truss finite element model

Table 5 Analytical natural frequencies

Mode	1	2	3	4	5
Healthy	19.88	38.31	66.26	67.17	92.25
Damaged	19.19	38.35	63.58	66.30	90.96

Table 6 Experimental healthy natural frequencies

Mode	1	2	3	4	5
Wn	20.65	41.49	64.59	69.41	95.51

An initial off-line modal identification is performed to accurately capture the dominant longitudinal bending modes of the healthy system i.e., the system with no damage. The eigensystem realization algorithm (ERA) (Juang and Pappa 1985) is used here to perform the modal identification analysis using forced response data. An electromagnetic shaker that can generate a maximum force of 20 lb and having a bandwidth of 5-9000 Hz is used to vertically excite the structure. A command input characterized by a band-limited white noise up to 256 Hz is applied to this shaker. Output data is acquired using six wired accelerometers mounted on the front panel, each measuring vertical response data with a sampling frequency of 512 Hz. Additionally, input signal measurement is obtained using a force transducer, located between the shaker and the structure. This test is performed with the full set of eleven wireless sensors attached to the truss to ensure that the mass distribution is identical before and after damage is applied to the system. System transfer functions are obtained and converted to impulse response functions. The ERA is applied to the impulse response functions to detect the first five dominant frequencies. The natural frequencies (in Hz) associated with the first five dominant bending modes of the healthy structure are given in Table 6. These values are to be used in the java tool that computes the final DLAC values. Note that these healthy natural frequencies are not obtained using the wireless sensors, and thus some additional experimental errors are introduced, demonstrating the robustness of the technique.

Damage is then introduced in the experimental truss by exchanging the indicated members to validate the proposed distributed SHM system. Impact testing, represented as $\delta(t)$ in Fig. 11, is employed to perform the validation by disconnecting the electromagnetic shaker and applying a hammer strike perpendicular to the longitudinal axis of the truss. Due to malfunctions in the drivers of the accelerometer, only 6 of the 11 sensors reported acquisition of raw data. The results obtained by the SHM system are provided in Table 7 and Fig. 13. The results indicate that the highest DLAC values are at the damaged positions. Here it is demonstrated that the approach is able to localize damage correctly even though modeling errors are present in the frequency change vectors.

Additional off-line analysis is conducted using the experimental data. Various assumed damage patterns are used in these off-line studies to evaluate the robustness of the approach. Here, additional assumed damage levels are considered and the experimentally obtained values for the healthy and damaged natural frequencies are used for DLAC correlation. Here each analytical damage scenario is simulated by replacing the set of 6 members in each bay with elements having a reduced area (see Fig 14). To generate the frequency vectors associated with the damage

Table 7 Identified natural frequencies (Hz)

Mode	WS #32	WS #45	WS #67	WS #28	WS #35	WS #75
1	20.2718	20.2795	20.1952	20.1685	20.3122	20.2254
2	41.3708	41.4002	41.2871	41.2315	41.2998	41.2947
3	63.0427	63.1657	63.0138	63.0467	63.1021	63.0198
4	67.7883	67.8858	67.6658	67.6792	67.7284	67.6820
5	94.8858	95.0803	94.8184	94.7336	94.8865	94.8080

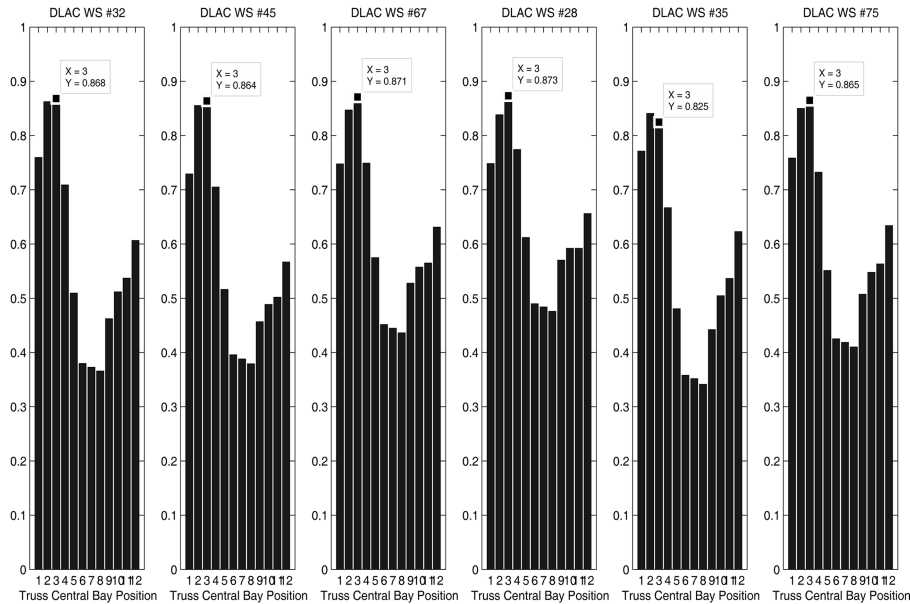


Fig. 13 DLAC results for truss bay # 3

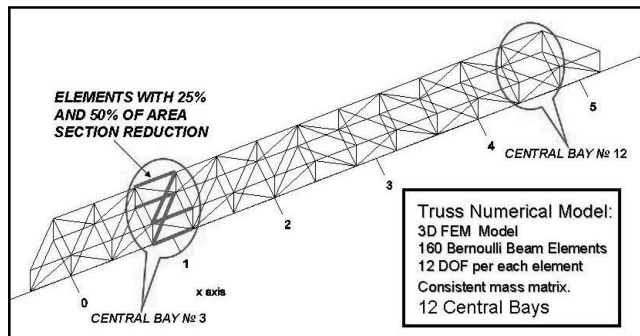


Fig. 14 Truss finite element model

hypotheses, the analytical model is modified by using elements with 25% and 50% reductions in the elemental cross-sectional areas of damaged members. Because the damage in the experimental structure is in the third bay, the highest correlation results are expected to be concentrated around to that position. The DLAC results of this off-line study are shown in Figs. 15 and 16.

The highest correlation values are concentrated between the first and third bay. Thus, even though the hypotheses are very different than the actual damage, the damage zone is determined with only five natural frequencies. The results for the case considering a 25% reduction (Fig. 15) show a symmetric pattern in the DLAC values corresponding to the three first and three last bays. This tendency can be explained by the nearly perfect symmetry of the structure. Therefore, DLAC approach is shown to be capable of detecting the most likely damage zones. Perhaps, if additional information is needed, this low power approach would be used for detecting damage zones, and a secondary level of analysis that requires more resources would be used to follow up.

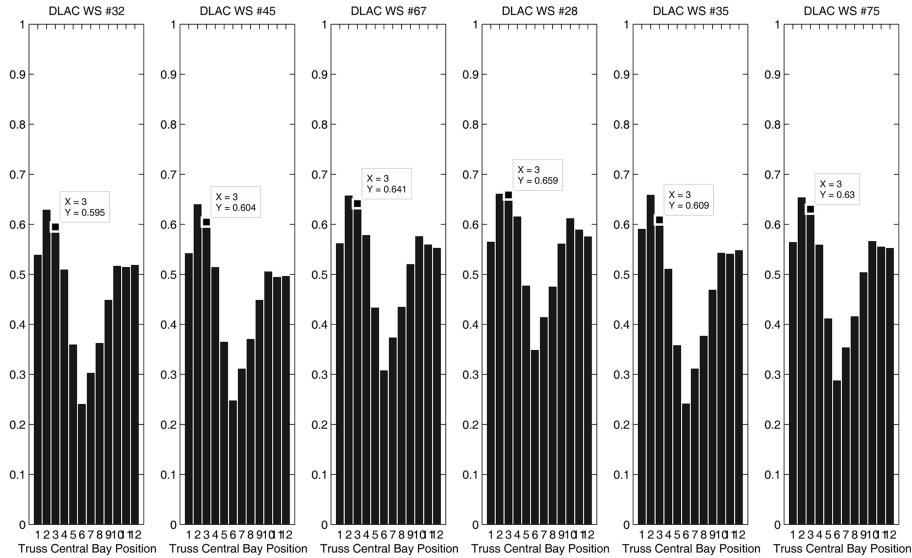


Fig. 15 DLAC results for truss bay # 3 under 25% of area section reduction

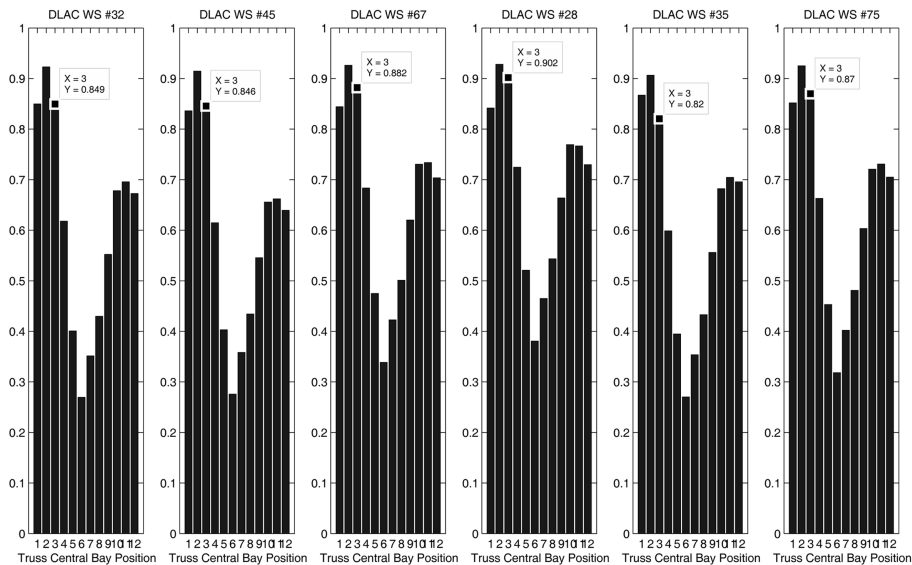


Fig. 16 DLAC results for truss bay # 3 under 50% of area section reduction

Additional analytical studies are performed in this section to validate the robustness of the DLAC method under different damage locations. A simulation, using the analytical model, is implemented in MATLAB (MathWorks 2006) to independently analyze two alternate damage positions with assumed damage levels corresponding to 25% and 50% reductions in the cross-sectional area. An equally spaced deployment of sensors is assumed in this study where the network of eleven sensor platforms is positioned along the frontal panel of the truss. The description of the cases considered is shown in Fig. 17.

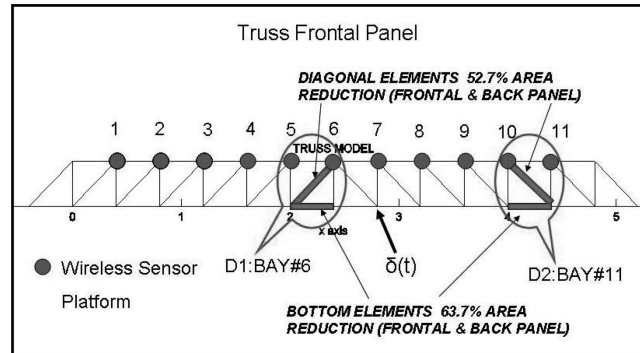


Fig. 17 Numerical simulation set up

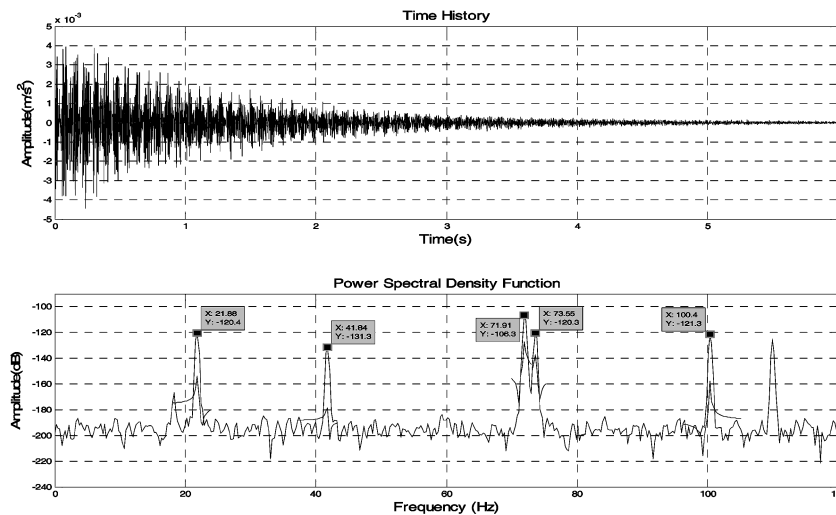


Fig. 18 Typical acceleration time history and corresponding power spectrum

The conditions used in the actual experiments are simulated in these numerical studies. Therefore, a sampling frequency of 560 Hz and corresponding cutoff frequency of 140 Hz are defined for each sensor to measure vertical acceleration data. Thus, to produce accurate results, the simulation time step is set to 1/5600sec and resampling is applied to the output to generate raw data sensed at the appropriate sampling frequency. The input is generated by the use of an impulse function, represented as $\delta(t)$ in Fig. 17, to approximate the effect of an impact testing. Physical uncertainties in the experimental model and data measurement errors involved in a true experiment are also simulated to produce *experimental* natural frequencies under more real conditions (Clayton 2006). Sensor noise is considered, defined as a bandlimited white noise with a magnitude of 10% of the standard deviation of the output signal. A non-homogeneous distribution of elemental densities and elastic moduli among the truss members are included to represent modeling errors. The same data processing is used as in the experimental implementation, involving the curve fitting technique, is performed over the raw data. Consequently, numerical values for the *experimental* healthy and damaged natural frequencies are obtained in a range of 8-10% of the analytical natural frequencies. A typical acceleration time history and corresponding power spectrum reported by one of the

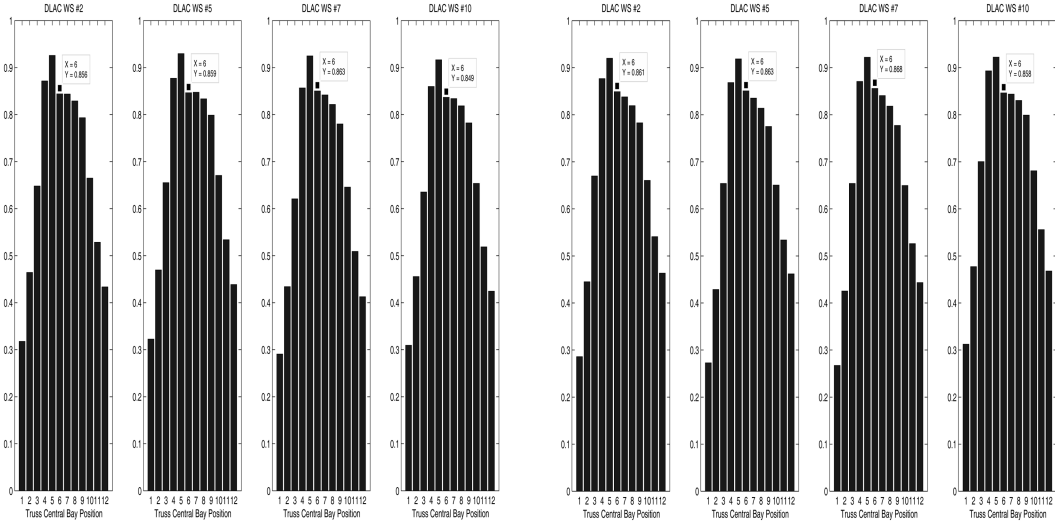


Fig. 19 DLAC results for truss bay #6 under 25% and 50 % of area section reduction

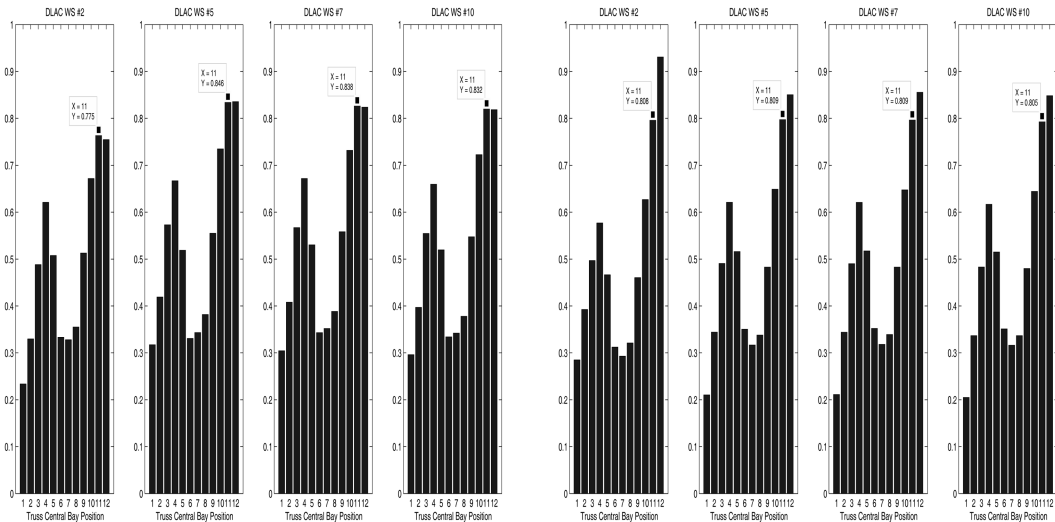


Fig. 20 DLAC results for truss bay #11 under 25% and 50% of area section reduction

sensors is depicted in Fig. 18. Damage is induced under the same conditions and configuration as the true damage imposed on the truss. Each damage scenario, D1 and D2, is associated with truss bays # 6 and # 11 respectively, as shown in Fig. 17. Therefore, the highest correlation values are expected to be concentrated around the sixth and eleventh bay because damage is located at these positions.

Results depicted in Fig. 19 and Fig. 20 show the calculated DLAC values. Due to space limitations, four representative sensor outputs are shown for each damage case (25% damage assumption- left plot and 50% damage assumption - right plot shown in each figure). The results of the first case (D1) indicate that structural damage is concentrated between the fourth and sixth bays. In the second case (D2) the results indicate that structural damage is concentrated between the

eleventh and twelfth bays. Therefore, both results are considered successful because the most likely damage zones have been detected with very different hypotheses than the actual damage and using only five natural frequencies. Thus, the results of the numerical studies are consistent with the experimental studies in detecting damage at different positions.

4. Conclusions

Damage detection systems based on distributed processing using minimal communication between smart sensor nodes are necessary to fully exploit the on-board processing capacity offered by smart sensors. In this study a distributed damage detection system is successfully deployed and experimentally validated using a smart sensor network. Two experimental structures of different complexities are tested. Experimental results and off-line analytical studies considering various damage level hypotheses demonstrated the potential of this system to identify likely damage zones. A 98.8% reduction in the amount of data transmitted, along with a 64.8% and 70.0% reduction in latency and energy usage, respectively, is achieved, resulting in a power efficient system. In some cases where damage localization is all that is needed, this system may operate alone. In other applications where damage quantification is needed, this system would be implemented as part of a multi-step procedure where it is followed by a secondary analysis that may require significantly more power for communication needs. Although it is not a focus of this study, the effects of temperature should also be considered in future examinations of this algorithm.

Acknowledgements

Funding for this research is provided in part by the National Science Foundation; grant NSF NeTS-NOSS Grant (CNS-0627126), NSF CRI Grant (CNS-0708460), and by Washington University in St. Louis. Additionally, the authors would like to thank Prof. Bill Spencer and Shin-Ae Jang for the use of and assistance with the experimental truss.

References

- Adler, R., Flanigan, M., Huang, J., Kling, R., Kushalnagar, N., Nachman, L., Wan, C.Y. and Yarvis, M. (2005), "Intel mote 2: An advanced platform for demanding sensor network applications", *Proc. 3th Int. Conference on Embedded Networked Sensor Systems*, 298-298.
- Bernal, D. (2002), "Load vectors for damage localization", *J. Eng. Mech.*, **128**(1), 7-14.
- Chintalapudi, K., Paek, J., Gnawali, O., Fu, T., Dantu, K., Caffrey, J., Govindan, R. and Jonson, E. (2006), "Structural damage detection and localization using NetSHM", *Proceedings of IPSN'06*, April 19-21, Nashville, Tennessee.
- Clayton, E.H. (2002), "Development of an experimental model for the study of infrastructure preservation", *Proceedings of the National Conference on Undergraduate Research*, Whitewater, Wisconsin.
- Clayton, E.H., Koh, B.H., Xing, G., Fok, C.L., Dyke, S.J. and Lu, C. (2005), "Damage detection and correlation-based localization using wireless mote sensors", *Proceedings of '05 The 13th Mediterranean Conference on Control and Automation*, Limassol, Cyprus.
- Clayton, E.H., Qian, Y., Orjih, O., Dyke, S.J., Mita, A. and Lu, C. (2006), "Of-the-shelf modal analysis: Structural health monitoring with motes", In *Proceedings of the 24th International Modal Analysis Conference*.

- Clayton, E.H. (2006), *Frequency Correlation-based Structural Health Monitoring with Smart Wireless Sensors*, Master of Science Thesis, Washington University in St. Louis.
- Contursi, T., Messina, A. and Williams, E.J. (1998), "A multiple-damage location assurance criterion based on natural frequency changes", *J. Vib. Control*, **4**, 619-633.
- Crosbow Technologies iMote2 Mote IPR2400 (2007), <http://www.xbow.com/Products/productdetails.aspx?sid=253>.
- Elson, J., Girod, L. and Estrin, D. (2002), "Fine-grained network time synchronization using reference broadcast", *Proc., 5th Symposium on Operating Systems Design and Implementation*, Boston, MA.
- Ferzli, N.A., Sandburg, C.J., King, T., Pei, J.S., Zaman, M.M., Refai, H.H., Ivey, R.A. and Harris, O. (2006), "Experimental investigation of 'smart dust' for pavement condition monitoring", *Proceedings of the 24th International Modal Analysis Conference (IMAC XXIV)*, St. Louis, MO, January 30 - February 2.
- Ganerwal, S., Kumar, R. and Srivastava, M.B. (2003), "Timing-sync protocol for sensor networks", *Proc., 1st International Conference on Embedded Networked Sensor Systems*, Los Angeles, CA, 138-149.
- Gangone, M.V., Whelan, M.J., Janoyan, K.D., Cross, K. and Jha, R. (2007), "Performance monitoring of a bridge superstructure using a dense wireless sensor network", *Proceedings of the 6th International Workshop on Structural Health Monitoring*, Stanford, California.
- Gao, Y. (2005), "Structural health monitoring strategies for smart sensor networks", Doctor of Philosophy Thesis, The University of Illinois at Urbana-Champaign.
- Hackmann, G., Sun, F., Castaneda, N., Lu, C. and Dyke, S. (2008), "A holistic approach to decentralized structural damage localization using wireless sensor networks", *Proceedings of the Real-time Systems Symposium*, 2008.
- Juang, J.N. and Pappa, R.S. (1985), "An eigensystem realization algorithm for modal parameter identification and model reduction", *J. Guid. Control Dyn.*, **8**, 620-627.
- Kim, S. (2005), "Wireless sensor networks for structural health monitoring", Master's thesis, University of California at Berkeley.
- Kim, S. (2007), "Wireless sensor networks for high fidelity sampling", Ph.D. Dissertation, University of California at Berkeley.
- Kim, S., Pakzad, S., Culler, D., Demmel, J., Fennes, G., Glaser, S. and Turon, M. (2007), "Health monitoring of civil infrastructures using wireless sensor networks", In *the Proceedings of the 6th International Conference on Information Processing in Sensor Networks (IPSN '07)*, Cambridge, MA, April 2007, ACM Press, 254-263.
- Koh, B.H. and Dyke, S.J. (2007), "Structural damage detection in cable-stayed bridges using correlation and sensitivity of modal data", *Comput. Struct.*, **85**, 117-130.
- Levy, E.C. (1959), "Complex-curve fitting", *IEEE T. Automat. Contr.*, **4**, 37-44.
- Liu, S.C. and Tomizuka, M. (2003), "Vision and strategy for sensors and smart structures technology research", In *Proceedings of the 4th International Workshop on Structural Health Monitoring*, Standford, CA, September 15-17, 42-52.
- Lynch, J.P., Kiremidjian, A.S., Law, K.H., Kenny, T. and Carryer, E. (2002), "Issues in wireless structural damage monitoring technologies", *The Proceedings of the Third World Conference on Structural Control*, **2**, 667-672.
- Lynch, J.P., Sundararajan, A., Law, K.H., Kiremidjian, A.S. and Ed Carryer. (2004), "Embedding damage detection algorithms in a wireless sensing unit for operational power efficiency", *Smart Mater. Struct.*, **13**, 800-810.
- Lynch, J.P. (2004), "Overview of wireless sensors for real time health monitoring of civil structures", In *Proceedings of the 4th International Workshop on Structural Control*, June 2004, 189-194.
- Lynch, J.P., Wang, Y., Law, K.H., Yi, J.-H., Lee, C.G. and Yun, C.B. (2005), "Validation of a large-scale wireless structural monitoring system on the Geumdang bridge", *Proc., the Int. Conference on Safety and Structural Reliability*, Rome, Italy.
- Lynch, J.P. and Loh, K. (2006), "A summary review of wireless sensors and sensor networks for structural health monitoring", *Shock and Vibration Digest*, in press.
- Maroti, M., Kusy, B., Simon, G. and Ledeczi, A. (2004), "The flooding time synchronization protocol", *Proc., 2nd International Conference On Embedded Networked Sensor Systems*, Baltimore, MD, 39-49.
- Mechitov, K.A., Kim, W., Agha, G.A. and Nagayama, T. (2004), "High-frequency distributed sensing for

- structure monitoring”, *Proc., 1st Int. Workshop on Networked Sensing Systems*, Tokyo, Japan, 101-105.
- Messina, A., Jones, I.A. and Williams, E.J. (1996), “Damage detection and localization using natural frequencies changes”, *Proceedings of Conference on Identification in Engineering Systems, Swansea, U.K.*, 67-76.
- Messina, A., Williams, E.J. and Contursi, T. (1998), “Structural damage detection by a sensitivity and statistical-based method”, *J. Sound Vib.*, **216**(5), 791-808.
- Nagayama, T., Rice, J.A. and Spencer, B.F. Jr. (2006), “Efficacy of Intel’s Imote2 wireless sensor platform for structural health monitoring applications”, *Proceedings of Asia-Pacific Workshop on Structural Health Monitoring*, Yokohama, Japan.
- Nagayama, T. (2007), “Structural health monitoring using smart sensors”, Doctor of Philosophy Thesis, The University of Illinois at Urbana-Champaign.
- Pakzad, S.N., Kim, S., Fenves, G.L., Glaser, S.D., Culler, D.E. and Demmel, J.W. (2005), “Multi-purpose wireless accelerometers for civil infrastructure monitoring”, *Proceedings of the 5th International Workshop on Structural Health Monitoring (IWSHM 2005)*, Stanford, CA.
- Pei, J.S., Ivey, R.A., Lin, H., Landrum, A.R., Sandburg, C.J., Ferzli, N.A., King, T., Zaman, M.M. and Refai, H.H., “Development and validation of “smart dust” for pavement condition monitoring”, *Journal of Intelligent Material Systems and Structures*, (submitted in December 2006, JIMSS-06-101).
- Rice, J.A., Mechtov, K.A., Spencer, Jr., B.F. and Agha G.A. (2008), “A service-oriented architecture for structural health monitoring using smart sensors”, *Proceedings of the 14th World Conference on Earthquake Engineering*, Beijing, China.
- Sohn, H., Farrar, C.R., Hemez, F.M., Shunk, D.D., Stinemas, D.W. and Nadler, B.R. (2004), “A review of structural health monitoring literature from 1996-2001”, Los Alamos National Laboratory report LA-13976-MS.
- Spencer, Jr., B.F. (2003), “Opportunities and challenges for smart sensing technology”, *First International Conference on Structural Health Monitoring and Intelligent Infrastructure*, Tokyo, 13-15 November 2003.
- Spencer, Jr., B.F. and Nagayama, T. (2006), “Smart sensor technology: a new paradigm for structural health monitoring”, *Proc., Asia-Pacific Workshop on Structural health Monitoring*, Yokohama, Japan.
- STMicroelectronics. (2005), LIS3L02DQ data Sheet <http://www.st.com/stonline/products/literature/od/10175/lis3l02dq.pdf>
- The Illinois SHM Services Toolkit (2008), <http://shm.cs.uiuc.edu/software.html>
- The MathWorks (2007), <http://www.mathworks.com/>
- TinyOS: <http://www.tinyos.net/>
- Zimmerman, A., Shiraishi, M., Swartz, A. and Lynch, J.P. (2008), “Automated modal parameter estimation by parallel processing within wireless monitoring systems”, *J. Infrast. Syst.*, ASCE, 2008.